



Investigation of thermal conductivity, sound absorption, and mechanical properties of *Alcea Rosea* L. fiber-reinforced epoxy composites

Seyda Eyupoglu¹ · Ertugrul Cetinsoy² · Can Eyupoglu³ · Nigar Merdan⁴

Received: 18 September 2023 / Revised: 25 October 2023 / Accepted: 29 October 2023
© The Author(s), under exclusive licence to Springer-Verlag GmbH Germany, part of Springer Nature 2023

Abstract

The composite production has been commonly researched because of its crucial properties such as low density, light weight, having better mechanical behaviors, and stiffness. There are numerous uses in marine, automotive, sporting, and aerospace industries. In this study, fiber-reinforced composites were produced with *Alcea Rosea* L. fiber and epoxy resin. Besides, an image processing technique was proposed and put into use to specify the average fiber thickness of *Alcea Rosea* L. fiber. The composites were prepared at 5:95, 10:90 fiber:epoxy resin weight percentages. Before the composite synthesis, *Alcea Rosea* L. fibers were treated to alkali surface modification with 10% sodium hydroxyl for 30 min. The thermal conductivity coefficient, sound absorption coefficient, and tensile strength of composites were measured. The thermal conductivity coefficient of samples decreases with increase in *Alcea Rosea* L. fiber weight percentage. The sound absorption coefficient and mechanical properties of samples improve with increase in *Alcea Rosea* L. fiber weight percentage. These results show that *Alcea Rosea* L. fiber-reinforced sustainable composites can be used as a potential thermal and acoustic insulator.

Keywords *Alcea Rosea* L. fiber · Epoxy resin · Fiber-reinforced composite · Thermal conductivity · Sound absorption · Tensile strength · Image processing

1 Introduction

Cellulosic fibers from natural resources are increasingly used as reinforcement material for developing polymer matrix-based composites as a result of rising environmental awareness and environmental regulations, which have prompted a focus on eco-friendly materials for a variety of industrial and domestic applications [1]. In literature, it is emphasized that these fibers have a variety of perfect properties which are

biodegradability, low cost, high-specific strength, renewability, capacity of carbon dioxide absorption, high mechanical properties, and consumption less energy. For these advantages of cellulosic fibers, many researchers were focalized on cellulosic fiber-reinforced composites and to successfully utilize them as reinforcement in composites [2]. Several plant-based natural fibers which are *Acacia nilotica* L. [3], *Zingiber Officinale* [4], *Strelitzia reginae* [5], *Thespesia populnea* [6], *Abutilon Indicum* [7], Lavender [8], Calamus manan [9], *Sambucus ebulus* L. [10], and *Brassica oleracea* var. *Italic* [11] have been investigated as a potential reinforcement in composite materials [12].

Epoxy resins, known as low molecular weight polymers, are a type of thermoset polymers involved covalent bonds. Recently, researchers have focused on epoxy resin because of high mechanical behaviors, chemical resistance, heat resistance, and high adhesiveness. Epoxy resin has been utilized in many applications which are painting, coating, encapsulating, fiber-reinforced composites, advanced composites, and broad materials [13].

Composites are commonly accepted as engineered materials consist of two or further constituents

✉ Seyda Eyupoglu
seyda.eyupoglu@istanbul.edu.tr

¹ Department of Textile, Clothing, Footwear and Leather, Vocational School of Technical Sciences, Istanbul University-Cerrahpasa, Istanbul, Turkey

² Department of Mechatronics Engineering, Technology Faculty, Marmara University, Istanbul, Turkey

³ Department of Computer Engineering, Turkish Air Force Academy, National Defence University, Istanbul, Turkey

⁴ Department of Fashion and Textile Design, Architecture and Design Faculty, Istanbul Commerce University, Istanbul, Turkey

(reinforcement and matrix material). Every constituent frequently comprises different chemical and physical properties. On a macroscopic level, within the finished construction, both constituents in a given composite material continue to be distinct and separate. Composite materials have been utilized since prehistoric times by many civilizations, and most famous example contains the bricks prepared with the use of mud and straw. The matrix in polymer composite materials serves as reinforcement, which can range from inorganic to organic components. Fibers, specifically all properties of composites, have been usually used as a reinforcement. The matrix also keeps the reinforcement and aids in load distribution along the reinforcement. Polymer composites are typically categorized based on the type of reinforcement. Polymer composites can be divided into fiber and particle-reinforced composites depending on the type of reinforcement used. Especially, the interest in the use of cellulosic fibers as reinforcement increases due to better studying conditions. Natural fibers have several benefits over their synthetic equivalents, but they also have a few drawbacks such as their hydrophilic nature and sensitive to moisture absorption. Depending on the applications, chemical treatments can be used to remedy the majority of drawbacks [14].

Plant-based fiber-reinforced composites has been commonly used in the automotive industry. It is reported that 75% of fuel consumption is directly related to vehicle weight, and every 10% decrease in vehicle weight results in an increase in fuel efficiency of 6–8%. Every 100 kg of weight saved in an automobile reduces CO₂ emissions by about 20 g/km for regularly used powertrains. European automobile manufacturers support the reduction of vehicle weight with using composites. Plant-based fiber-reinforced composites are generally utilized in interior parts of automobiles due to relatively low mechanical behaviors and intrinsic moisture sensitivity. New examples of plant-based fiber-reinforced composites application include abaca-reinforced composites for fender components, flax/vinyl ester composites for automobile hoods, kenaf/epoxy composites for spall liners, bamboo/polyurethane composites for acoustic insulator for door panels, flax/Acrodur composites for fast molding parts in automobile [12].

The main aim and contribution of this study is to manufacture *Alcea Rosea L.* plant stem fiber reinforced epoxy resin composite. To the best of authors' knowledge, there is no other research in literature on a new composite material reinforced with *Alcea Rosea L.* plant stem fiber. In this study, plant-based fibers were successfully extracted from *Alcea Rosea L.* plant stem of 592.14- μm thickness. The obtained fibers were treated with surface

modification with 10% sodium hydroxyl (NaOH). After, *Alcea Rosea L.* (ARL) fiber-reinforced composites were manufactured with using epoxy resin polymer matrix via hand lay-up technique. The composites were produced at 5:95, 10:90 fiber: resin weight percentages. The thermal conductivity coefficient, sound absorption coefficient, density, and tensile strength of composites were analyzed in terms of fiber:resin weight percentages. According to the results, the density of ARL fiber-reinforced composites decreases with increase in ARL fiber weight percentage. The thermal conductivity coefficient of samples diminishes with rising of ARL fiber weight percentage. The sound absorption coefficient and mechanical properties of samples improve with increase in ARL fiber weight percentage. These results show that sustainable ARL fiber-reinforced composites can be used in many areas such as buildings and vehicles.

2 Materials and methods

2.1 Materials

In the natural fiber-based reinforced epoxy resin composites, *Alcea rose L.* fiber was utilized as reinforcement and epoxy resin was used as matrix. *Alcea rosea L.* often reaches heights of 2 to 2.5 m. *Alcea Rosea L.* stems were cultivated from the Black Sea Region, Sakarya, Turkey, in June 2020. For 3 weeks, the stems were submerged in water to promote microbial degradation. The outer layer of the plant's stem becomes soft after microbial deterioration, and the fibers are manually collected. The fibers (Fig. 1) were then dried for a week in direct sunlight. *Alcea Rosea L.* fiber was



Fig. 1 The image of ARL fiber [15]

Table 1 *Alcea Rosea* L. fiber characteristic properties

	Density (g/cm ³)	Thickness (μm)	Crystallinity index (%)	Crystallinity size (nm)	Thermal degradation temperature (°C)	Tensile strength (MPa)	Young's mod- ule (GPa)	Elongation at break (%)
ARL fiber	0.45	592.14	80	3.89	361.39	80.96	3.28	2.47

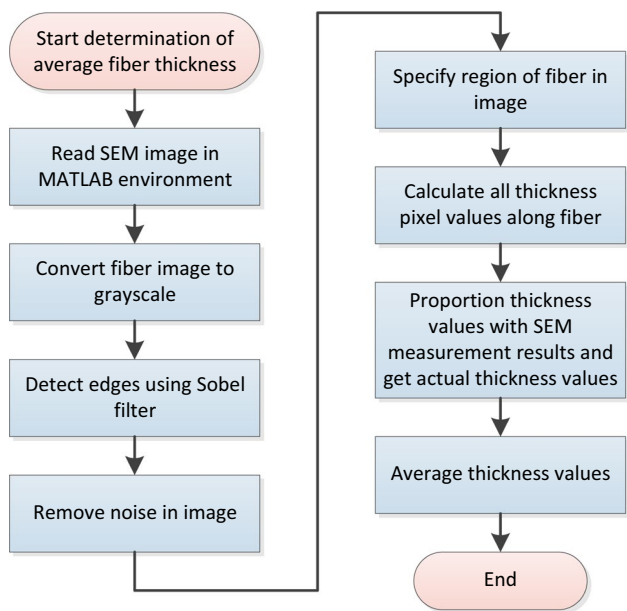


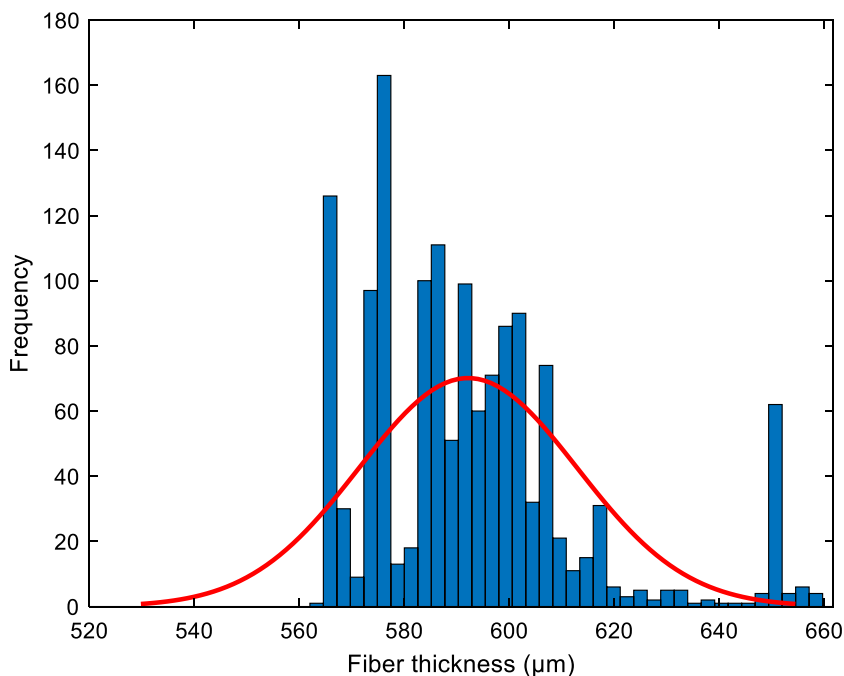
Fig. 2 Flowchart of the proposed image processing technique

characterized in our previous study and the results was summarized in Table 1 [15].

The fiber thickness of the ARL fiber was measured using an electron microscope that renders images of the fibers in longitudinal direction. The average fiber thickness was determined in this work utilizing a new image processing technique proposed using images from an electron microscope. The flowchart of the proposed technique is shown in Fig. 2.

As shown in the flowchart, firstly, the SEM image of the ARL fiber is read in the MATLAB environment. The fiber image is converted to grayscale. An edge detection process is applied using the Sobel filter, and then the noise in the image is removed. Afterwards, the region of the fiber in the image is specified, and all thickness pixel values along the fiber are calculated. Subsequently, the thickness values are proportioned with the reference SEM thickness results, and the actual thickness values are attained. Finally, the average fiber thickness is computed for the selected ARL fiber. The average fiber thickness was calculated using the proposed image processing technique to be 592.14 μm. The thickness histogram of the ARL fiber is demonstrated in Fig. 3.

Fig. 3 The thickness histogram of ARL fiber



2.2 Method

2.2.1 Surface modification

In order to improve the adhesion between fibers and epoxy resin, ARL fibers were treated with 10% NaOH for 30 min at room temperature. The surface modification was performed by a conventional method in a bath ratio of 1:50. Then the fibers were washed with distilled water to remove NaOH. Then fibers were sun-dried for 8 h and were then oven dried at 50 °C for 2 h.

2.2.2 Manufacturing of composites

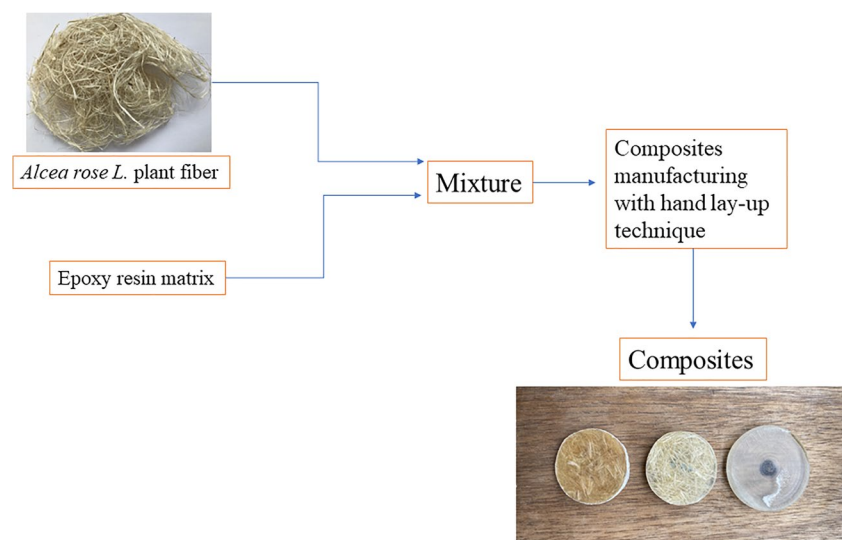
In order to manufacture composite parts, initially, molds are produced by machining block material according to the desired size and shape. Four different molds are produced for test samples with the shapes of a 100 × 120 × 20-mm rectangle, 25 cm long 4-mm thick dog bone, and 4-mm thick circles with $\Phi = 25$ mm and $\Phi = 29$ mm. For the test samples, molds are produced using PTFE, which is a material with very low adhesion, for facilitating the demolding process. Before molding, a mixture of epoxy resin and fibers is prepared with strict weight ratio by using a weight scale with precision of 0.1 g. For the test samples, Resinin Mass Lite epoxy with 2:1 resin-stiffener weight ratio and 24-h curing time is used. This epoxy resin is preferred for its transparency, which allows easy detection of any manufacturing defects. Also due to its long curing time, relatively slow reaction of the epoxy allows the heat dissipation rate in a thermally insulated mold made of PTFE to be similar to the heat generation rate, so heat accumulation that expands the epoxy resin is prevented. The mixture shrinks during curing. In order to obtain parts with the thickness of the mold, the prepared mixture is poured

into the mold with some overshoot, which is allowed by the surface tension of the epoxy. After demolding, sample parts are trimmed to the demanded thickness. Rectangle sample part with 100 × 120 × 20 mm dimensions is molded in three steps with approximately 7-mm thickness at each step. The thickness at each step is limited to prevent non-homogenous distribution of resin and fiber due to the density difference and to prevent expansion of the epoxy especially near the bottom of the mold due to thick upper cover and PTFE undercover. The manufacturing process is summarized in Fig. 4.

2.2.3 Sound absorption coefficient measurement

Sound absorption coefficient of composites was gauged with Brüel & Kjaer Impedance Tube instrument according to ISO 10534-2 [16] standard. Brüel & Kjaer Impedance Tube involves of two tubes having 2.9-cm and 10-cm diameters. The bigger tube was used to measure the material in the frequency range of 0–1600 Hz, while the smaller tube was used to measure the material in the frequency range of 600–6300 Hz. A loudspeaker was positioned at one end of the tube to serve as a sound source, and the material was placed at the other end of the tube. Some of the waves sent from the loudspeaker to the material are absorbed by the material and some are reflected by the material. The reflected waves are measured by the microphone. The ratio between the amount of incident wave and the amount of reflected wave expresses the sound absorption coefficient of the material. The test substance was positioned at the other end of the tube to measure its ability to absorb sound. Three iterations of the sound absorption coefficient measurements were performed.

Fig. 4 Summary of the manufacturing process of composites



2.2.4 Thermal conductivity coefficient measurement

Thermal conductivity coefficients of samples were determined with using KEM QTM 500 instrument. The samples were prepared $120 \times 60 \times 20$ mm dimensions to tests. The thermal conductivity coefficient measurements were iterated three times.

2.2.5 Tensile property measurement

Tensile property of ARL-ERC was characterized based on ISO 6892–1:2019 standard method with 3 mm/min of crosshead movement at 25 °C room temperature. In order to determine the tensile properties of each sample, five different measurements were carried out and the average value was calculated.

3 Results and discussion

3.1 Thermal conductivity coefficient measurements

The thermal conductivity coefficient results of randomly oriented ARL fiber reinforced composites are given in Fig. 5.

The average thermal conductivity coefficient of ARL fiber-reinforced composites and epoxy matrix were 0.2510 W/m.K and 0.2877 W/m.K, respectively. According to Fig. 4, it is clearly shown that thermal conductivity coefficient of samples displays as a function of ratio of ARL fiber. Increase in ratio of ARL fiber in composites causes decrease in the thermal conductivity coefficient of samples. The thermal conductivity of composites has a decreasing behavior trend as the fiber ratio is increased, relative to the thermal

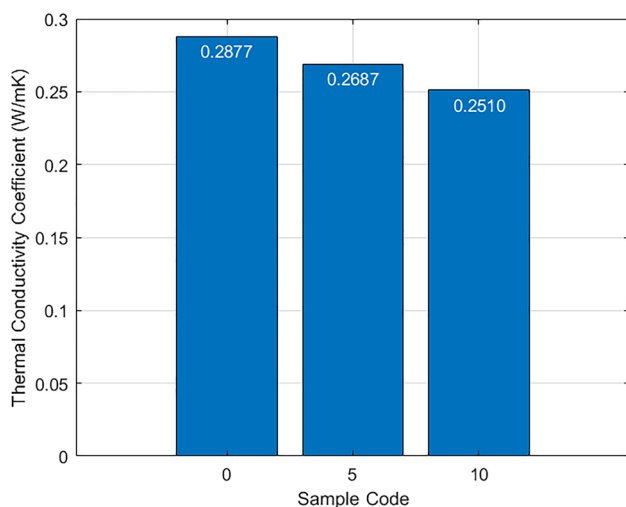


Fig. 5 Thermal conductivity coefficient results of randomly oriented ARL fiber reinforced composites

conductivity of the polymer matrix. The decreased heat conductivity of the fiber inserted in the polymer matrix appears to justify this behavior of polymer composites. At high fiber ratio, non-thermally conductive fibers can generate overlapping contacts and interconnecting network helpful for the heat path formation through the composites, decreasing in the thermal resistance. The greater the fiber volume, the larger of heat resistance routes shaped within the polymer matrix composite [17, 18]. Furthermore, the thermal conductivity behavior of composites varies in accordance with matrix polymer and fiber [19].

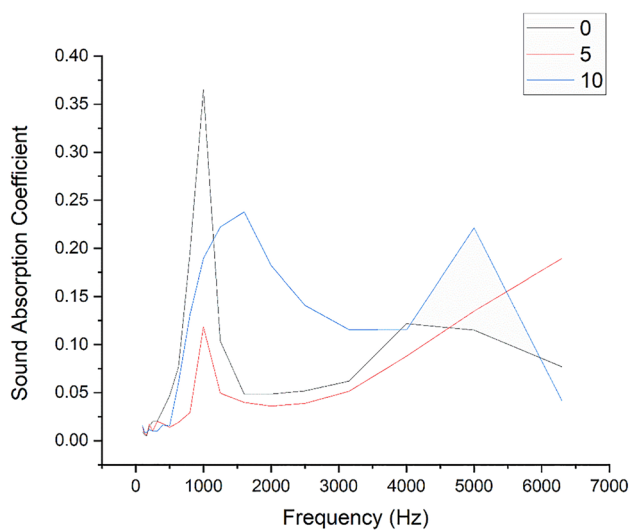
In literature, it is reported that polymer matrix plays a significant role in obtaining thermal conductivity of composites. Experimental research and molecular simulations have demonstrated that a polymer chain can have a relatively high thermal conductivity in theory [20]. Besides, the polymers, known as having bulk on macro scale, have low thermal conductivity coefficient. The difference between the thermal conductivity of bulk polymers and equivalent single chains is evident. Moreover, bulk polymers have voids, polymer chain ends, entanglements, and impurities which cause to reduce the thermal conductivity coefficient. Furthermore, crystalline polymers have high thermal conductivity coefficient compared with amorphous polymers like polyurethane. Lower thermal conductivity coefficient is typically the result of the addition of heavier atoms and the presence of side chains or pendant groups [21]. In addition, cellulose-based fibers have lumen layer extending along the longitudinal axis of the fiber and containing air. Lumen layer is known one of the main factors effected thermal conductivity coefficient of cellulose-based fibers. Besides, the fiber bundle's lumen serves as a heat-transmission barrier [22]. Thermal conductivity coefficients of some plant-based fiber reinforced composites are given in Table 2.

3.2 Sound absorption coefficient measurement

The sound absorption coefficient of a material is a quantity that describes how much of the incident sound intensity is not reflected by the material. Sound absorption coefficient of ARL-reinforced epoxy resin composites is given in Fig. 5. Upon consideration of the results with regards to ARL fiber fraction, sound absorption coefficient of the sample having 10% (wt) ARL fiber is higher than epoxy resin and 5% (wt) having ARL fiber reinforced epoxy resin composite. It is known that cellulose-based fibers have hollow lumen layer which cause the increase in the amount of air within the ARL-reinforced epoxy composite, whereas sound absorption coefficients of the composite increased with the increasing air fraction of composites [22]. The improvement in the sound absorption coefficient based on the reinforcement ratio may be owing to the large surface area of ARL fibers in the epoxy resin matrix, where sound waves can be

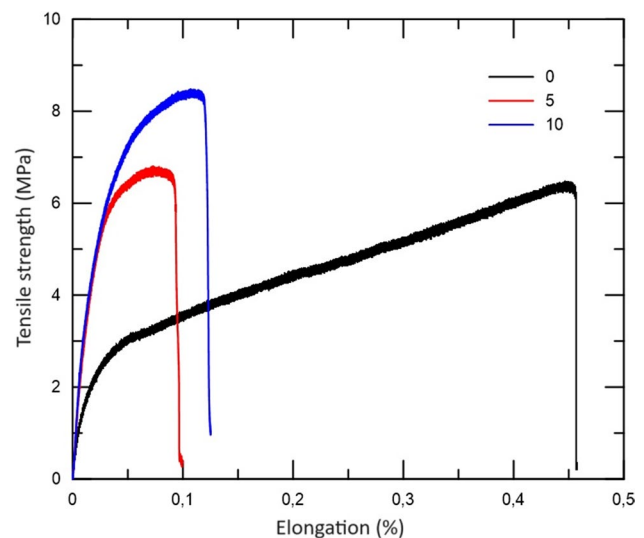
Table 2 Thermal conductivity coefficients of some plant-based fiber reinforced composites

Matrix	Reinforced	Reinforced loading (wt.%)	Thermal conductivity (W/m.K)	References
Epoxy/poly-lactic acid	Hemp fiber	76	0.19	[23]
Epoxy	Alginate graphene	1.7	2.13	[24]
Epoxy	Multi-layer graphene	5.7	1.5	[25]
Epoxy	Bamboo	40	0.345	[22]
Epoxy	Abaca	40	0.185	[22]
Polyester	<i>Typha angustifolia</i>	0.32 (volume %)	0.137	[26]
Polyester	<i>Calotropis procera</i>	10	0.166	[27]
Polyester	Banana/sisal	0.4 (volume %)	0.153	[28]
Polypropylene	Banana	0.10 (volume %)	0.217	[29]
Polypropylene	Banana	0.50 (volume %)	0.157	[29]
Epoxy resin	ARL	10	0.251	Recent study

**Fig. 6** Sound absorption coefficient of ARL-reinforced epoxy resin composites

transformed to heat energy depending on high frictions. Pore and cell size of composites, open, closed, or semi-open pores are significant factors effecting sound absorption coefficient of composites [30].

Furthermore, Fig. 6 indicates that the sound absorption coefficient of ARL-reinforced composites is higher at 5300–6000-Hz frequency than at low frequencies. The results demonstrate that the sound absorption coefficient of samples is lower at low frequencies. Low frequency sound waves have a long wavelength and a small amplitude, making it simple for them to pass over the sound waves in contacting surface from behind. Sound absorption coefficients of the ARL-fiber reinforced composites improved at 5300–6000 Hz as a result of the sound waves' shortened wavelengths and increased amplitudes. An increase in amplitude led to more interactions between sound waves and the absorbing surface, which changed the nature of sound

**Fig. 7** The tensile strength measurement result for the composites

waves into a loss of heat energy. Additionally, sound waves cause vibration in the pores of a fibrous material, increasing frictions, when they pass through the material [30].

3.3 Tensile property measurement

In this study, alkali treatment was performed to ARL fibers. It is known that alkali treatment causes to improve fiber surface roughness as resulting increase in adhesion between fibers and polymer matrix. The increase in adhesion between fiber and matrix increases in tensile strength of composite materials. The tensile strength measurement result for the composites involved different fiber content is indicated in Fig. 7.

Table 3 Tensile strength and density of some plant-based fiber composites

Reinforcement	Matrix polymer	Reinforced loading (wt %)	Density of composite (kg/m ³)	Mean tensile strength (MPa)	References
<i>Typha angustifolia</i>	Polyester	0.355 (volume %)	1010	48.92	[26]
<i>Ficus benjamina L</i>	Polyester	40	-	77.71	[31]
Banana	Polyester	51	-	59	[29]
Banana	Epoxy	-	-	47	[29]
Pineapple/flax	Epoxy resin	30	1197	23.04	[17]
Kenaf	Acrylonitrile butadiene styrene	2.5	-	321.73	[32]
Bamboo/polypropylene	Polypropylene	-	-	367.3	[22]
Cellulose nano fiber	Polyurethane	30	-	32	[22]
Jute	Epoxy resin	18	-	10.5	[33]
Jute	Polyester	18	-	12.46	[33]
Sisal	Polyester	16.11	0.99	29.66	[34]
ARL	Epoxy resin	10	750	8.5	Recent study

Figure 7 shows that tensile strength of epoxy resin improves with ARL fiber reinforcement. Associated with epoxy resin matrix, reinforcement and matrix can interlock and bind manufacturing composites with high mechanical behaviors when compared to un-reinforcement epoxy resin matrix. Furthermore, after NaOH surface treatment, chemical bonding between epoxy resin and treated ARL fiber was increased since ARL fiber surface allows to create many hydrogen bonds between epoxy groups and hydrogen groups of cellulose in fiber [1]. According to the results, it is determined that increasing in the ARL fiber content in the epoxy resin matrix, the tensile strength improves. This is owing to the fact that epoxy resin distributes and transmits the measurement stress to ARL fibers, resulting in a high strength. For this reason, the composite can tolerate higher load than unreinforced epoxy resin. At the highest fiber content (10 wt.%), it is discovered that the composites have a 41% higher tensile strength than pure epoxy resin. This proves the viability of creating novel composites including abundantly present in nature fiber from ARL for application in low-cost housing, civil engineering material, and vehicle panels [26]. Tensile strength and density of some plant-based fiber composites are summarized in Table 3. According to Table 3, tensile strength and density values of some plant-based fiber-reinforced composites are distributed over a wide range. The tensile property and density of ARL fiber-reinforced composite have approximate values to other plant-based fiber-reinforced composites.

4 Conclusions

In this study, *Alcea Rosea L.* fiber-reinforced epoxy polymer composites have been manufactured with hand lay-up technique. According to the thermal conductivity coefficient measurement result, it is clearly determined that thermal

conductivity coefficient of samples displays as a function of ratio of ARL fiber. Increase in ratio of ARL fiber in composites causes to decrease in the thermal conductivity coefficient of samples. The sound absorption coefficient measurement results show that sound absorption coefficient of the sample having 10 wt.% ARL fiber is higher than epoxy resin and 5 wt.% having ARL fiber-reinforced epoxy resin composite. According to tensile test, it was proved that increased in fiber content causes to increase in tensile strength of composites. The tensile strength also improved with an increased in the fiber content, the optimal tensile strength achieved at 10 wt.% was found to be 8.5 MPa. Furthermore, the elongation at break (%) improves with increased in fiber content an at 10 wt.%. In addition, it can be mentioned that these composites can be utilized in many technical areas which desired thermal and acoustic insulation. Plant-based materials can be used to increase in thermal and acoustic insulation without increase in the thickness of the materials. As a result, sustainable development in composite production will be encouraged and costs can be decreased.

Author contribution S.E. carried out thermal conductivity and sound absorption coefficient, mechanical behaviors of composite materials. E.C. produced composite materials. C.E. developed and implemented an image processing method to determine the average fiber thickness of ARL fiber. N.M. extracted the ARL fiber from plant stem and produced composite materials. All authors wrote and reviewed the main manuscript.

Data availability The data that support the findings of this study are available on request from the corresponding author. The data are not publicly available due to privacy or ethical restrictions.

Declarations

Ethics approval The authors confirm that there were no ethical in preparing this manuscript.

Consent to participate All authors consent to participating in this work.

Competing interests The authors declare no competing interests.

References

- Rajeshkumar G, Hariharan V, Indran S, Sanjay MR, Siengchin S, Maran JP, Al-Dhabi NA, Karuppiyah P (2021) Influence of sodium hydroxide (NaOH) treatment on mechanical properties and morphological behaviour of Phoenix sp. fiber/epoxy composites. *J Polym Environ* 29:765–774. <https://doi.org/10.1007/s10924-020-01921-6>
- Ramamoorthy SK, Skrifvars M, Persson A (2015) A review of natural fibers used in biocomposites: plant, animal and regenerated cellulose fibers. *Polym Review* 55(1):107–162. <https://doi.org/10.1080/15583724.2014.971124>
- Kumar R, Sivaganesan S, Senthamaraiannan P, Saravanakumar SS, Khan A, Ajith Arul Daniel S, Loganathan L (2022) Characterization of new cellulosic fiber from the bark of *Acacia nilotica* L. plant. *J Nat Fiber* 19(1):199–208. <https://doi.org/10.1080/15440478.2020.1738305>
- Eyupoglu S (2022) Characterization of new cellulosic fibers obtained from zingiber officinale. *J Nat Fiber* 19(4):1287–1296. <https://doi.org/10.1080/15440478.2020.1764452>
- Lemita N, Deghboudj S, Rokbi M, Rekbi FML, Halimi R (2022) Characterization and analysis of novel natural cellulosic fiber extracted from *Strelitzia reginae* plant. *J Compos Mater* 56(1):99–114. <https://doi.org/10.1177/00219983211049285>
- Pandiarajan P, Kathiresan M, Baskaran PG, Kanth J (2022) Characterization of raw and alkali treated new cellulosic fiber from the rinds of *Thespesia populnea* plant. *J Nat Fiber* 19(11):4038–4049. <https://doi.org/10.1080/15440478.2020.1852996>
- ArunRamnath R, Murugan S, Sanjay MR, Vinod A, Indran S, Elnaggar AY, Siengchin S (2023) Characterization of novel natural cellulosic fibers from *Abutilon Indicum* for potential reinforcement in polymer composites. *Polym Compos* 44(1):340–355. <https://doi.org/10.1002/pc.27100>
- Eyupoglu S, Merdan N (2022) Physicochemical properties of new plant-based fiber from lavender stem. *J Nat Fibers* 19(14):9248–9258. <https://doi.org/10.1080/15440478.2021.1982816>
- Ding L, Han X, Cao L, Chen Y, Ling Z, Han J, Jiang S (2022) Characterization of natural fiber from manau rattan (*Calamus manan*) as a potential reinforcement for polymer-based composites. *J Bioresources Bioprod* 7(3):190–200. <https://doi.org/10.1016/j.jobab.2021.11.002>
- Eyupoglu S, Eyupoglu C, Merdan N (2023) Physico-chemical characterization of *Sambucus ebulus* L. plant stem fiber. *Biomass Conv Bioref* 1–11. <https://doi.org/10.1007/s13399-023-04054-7>
- Eyupoglu S (2022) Characterization of a novel cellulosic fiber from brassica oleracea var. italic stem. *J Nat Fiber* 19(14):7480–7490. <https://doi.org/10.1080/15440478.2021.1950098>
- Li M, Pu Y, Thomas VM, Yoo CG, Ozcan S, Deng Y, Nelson K, Ragauskas AJ (2020) Recent advancements of plant-based natural fiber-reinforced composites and their applications. *Compos Part B: Eng* 200:108254. <https://doi.org/10.1016/j.compositesb.2020.108254>
- Kumar B, Roy S, Agumba DO, Pham DH, Kim J (2022) Effect of bio-based derived epoxy resin on interfacial adhesion of cellulose film and applicability towards natural jute fiber-reinforced composites. *Int J Biol Macromol* 222:1304–1313. <https://doi.org/10.1016/j.ijbiomac.2022.09.237>
- Thakur VK, Thakur MK (2014) Processing and characterization of natural cellulose fibers/thermoset polymer composites. *Carbohydr Polym* 109:102–117. <https://doi.org/10.1016/j.carbpol.2014.03.039>
- Eyupoglu S, Merdan N (2022) Investigation of the characteristic and sound absorption properties of a new cellulose-based fiber from *Alcea rose* L. plant. *J Nat Fiber* 19(15):10082–10093. <https://doi.org/10.1080/15440478.2021.1993481>
- ISO 10534–2 Standard (1998) Acoustics – determination of sound absorption coefficient and impedance in impedance tubes – Part 2: transfer-function method.
- Sumesh KR, Kanthavel K, Kavimani V (2020) Peanut oil cake-derived cellulose fiber: extraction, application of mechanical and thermal properties in pineapple/flux natural fiber composites. *Int J Biol Macromol* 150:775–785. <https://doi.org/10.1016/j.ijbiomac.2020.02.118>
- Kumar S, Locke J, McNally T (2023) Thermal conductivity of composites of polymers and 0D/1D/2D materials. *Encyclopedia of Nanomaterials* 1:730–753. <https://doi.org/10.1016/B978-0-12-822425-0.00119>
- Behzad T, Sain M (2007) Measurement and prediction of thermal conductivity for hemp fiber reinforced composites. *Polym Eng Sci* 47(7):977–983. <https://doi.org/10.1002/pen.20632>
- Henry A, Chen G (2008) High thermal conductivity of single polyethylene chains using molecular dynamics simulations. *Phys Rev Lett* 101(23):235502. <https://doi.org/10.1103/PhysRevLett.101.235502>
- Chen H, Ginzburg VV, Yang J, Yang Y, Liu W, Huang Y, Chen B (2016) Thermal conductivity of polymer-based composites: fundamentals and applications. *Prog Polym Sci* 59:41–85. <https://doi.org/10.1016/j.progpolymsci.2016.03.001>
- Liu K, Takagi H, Osugi R, Yang Z (2012) Effect of physico-chemical structure of natural fiber on transverse thermal conductivity of unidirectional abaca/bamboo fiber composites. *Compos Part A: App Sci Manufac* 43(8):1234–1241. <https://doi.org/10.1016/j.compositesa.2012.02.020>
- Osugi R, Takagi H, Liu K, Gennai Y (2009) Thermal conductivity behavior of natural fiber-reinforced composites. In: *Proceedings of the Asian Pacific Conference for Materials and Mechanics*, Yokohama, Japan
- Lian G, Tuan CC, Li L (2016) Vertically aligned and interconnected graphene networks for high thermal conductivity of epoxy composites with ultralow loading. *Chem Mater* 28:6096–6104. <https://doi.org/10.1021/acs.chemmater.6b01595>
- Shen X, Wang Z, Wu Y (2016) Multilayer graphene enables higher efficiency in improving thermal conductivities of graphene/epoxy composites. *Nano Lett* 16:3585–3593. <https://doi.org/10.1021/acs.nanolett.6b00722>
- Ramanaiah K, Ratna Prasad AV, Chandra Reddy KH (2011) Mechanical properties and thermal conductivity of *Typha angustifolia* natural fiber-reinforced polyester composites. *Int J Polym Anal Ch* 16(7):496–503. <https://doi.org/10.1080/1023666X.2011.598528>
- Nagaraja Ganesh B, Rekha B, Yoganandam K (2022) Assessment of thermal insulation and flame retardancy of cellulose fibers reinforced polymer composites for automobile interiors. *J Nat Fiber* 19(15):11021–11029. <https://doi.org/10.1080/15440478.2021.2009395>
- Idicula M, Devi U, Thomas S (2006) Thermo physical properties of natural fiber reinforced polyester composite. *J Compos Sci Technol* 66:27192725. <https://doi.org/10.1016/j.compscitech.2006.03.007>
- Venkateshwaran N, Elayaperumal A (2010) Banana fiber reinforced polymer composites-a review. *J Reinf Plast Compos* 29(15):2387–2396. <https://doi.org/10.1177/0731684409360578>

30. Canbolat S, Kut D, Dayioglu H (2015) Investigation of pumice stone powder coating of multilayer surfaces in relation to acoustic and thermal insulation. *J Ind Text* 44(4):639–661. <https://doi.org/10.1177/1528083713516665>
31. Joe M S, Sudherson D, Suyambulingam I, Siengchin S, Rajeshkumar G (2023) Characterization of novel cellulosic plant fiber reinforced polymeric composite from *Ficus benjamina* L. stem for lightweight applications. *Biomass Conv Bioref* 1–14. <https://doi.org/10.1007/s13399-023-04379-3>
32. Han S, Taha MM, Mansor MR, Rahman M (2022) Investigation of tensile and flexural properties of kenaf fiber-reinforced acrylonitrile butadiene styrene composites fabricated by fused deposition modeling. *J Eng Appl Sci* 69(1):52. <https://doi.org/10.1186/s44147-022-00109-0>
33. Gopinath A, Kumar MS, Elayaperumal A (2014) Experimental investigations on mechanical properties of jute fiber reinforced composites with polyester and epoxy resin matrices. *Pro Eng* 97:2052–2063. <https://doi.org/10.1016/j.proeng.2014.12.448>
34. Li Y, Mai YW, Ye L (2000) Sisal fiber and its composites: a review of recent developments. *Compos Sci Techno* 60(11):2037–2055. [https://doi.org/10.1016/S0266-3538\(00\)00101-9](https://doi.org/10.1016/S0266-3538(00)00101-9)

Publisher's note Springer Nature remains neutral with regard to jurisdictional claims in published maps and institutional affiliations.

Springer Nature or its licensor (e.g. a society or other partner) holds exclusive rights to this article under a publishing agreement with the author(s) or other rightsholder(s); author self-archiving of the accepted manuscript version of this article is solely governed by the terms of such publishing agreement and applicable law.